A dopant-free polymer as hole-transporting material for highly efficient and stable perovskite solar cells

Xianqiang Li, Xiaohong Tang, Yijie Yang, Tao Ye, Dan Wu, Hong Wang, Jun Li*, Xizu Wang**

X. Q. Li, T. Ye, Dr. J. Li, Dr. X. Z. Wang,
Institute of Materials Research and Engineering (IMRE)
Agency for Science, Technology and Research (A*STAR)
2 Fusionopolis Way, Innovis, #08-03, 138634, Singapore
E-mail: j-li@imre.a-star.edu.sg, wangxz@imre.a-star.edu.sg
X. Q. Li, Prof. X. H. Tang, D. Wu, Prof. H. Wang
School of Electrical and Electronics Engineering
Nanyang Technological University
50 Nanyang Avenue, 639798, Singapore
E-mail: exhtang@ntu.edu.sg
Y. J. Yang
Division of Chemistry and Biological Chemistry
School of Physical and Mathematical Sciences
Nanyang Technological University, 637371, Singapore
T. Ye
Department of Mechanical Engineering
National University of Singapore
21 Lower Kent Ridge Road, 119077, Singapore

Keywords: perovskite solar cell, hole-transporting material, stability, crystallinity

Abstract

A series of Thiazolothiazole-Thiophene based polymer hole-transporting materials (HTMs) are synthesized and applied into perovskite solar cells (PSCs). These polymer HTMs have good performance and stability without any dopants. The improved performance and stability of PSCs is attributed to the polymer HTMs' crystallinity which can be controlled by adjusting the thiophene units on the polymer backbone. The highest PCE of the polymer HTMs based PSCs reached 14.02%. The stability of the PSCs was shown by retaining 80% PCE of the original value after stored them in a N_2 filled glovebox for 113 days.

1. Introduction

Solution processed organic-inorganic lead halide perovskite solar cells (PSCs) have attracted a lot of attentions after experiencing a sky-rocketing increasing their power conversion efficiency (PCE) in recent years. Within 6 years, the PCE of PSCs has been enhanced from 3.8%[1] up to above 20%.[2-6]The dramatic PCE enhancement of the solar cells has never been seen before in any other photovoltaic technologies. Benefiting from the solution processibility, manufacturing costs of the PSCs are much lower when compared to that of other photovoltaic techniques based on inorganic materials such as silicon. The high PCE and low manufacturing costs make PSCs a promising candidate to compete with the current silicon dominated photovoltaic technology.

PSCs are normally with two different structures: mesoscopic structure and planar structure. In the mesoscopic structure PSCs, a mesoporous TiO_2 scaffold layer is used for fast extraction of electrons from the perovskite layer [7]. While the planar structure PSCs do not have the mesoporous TiO_2 scaffold layer, only a layer of compact TiO_2 [8] or other n-type materials, such as [6,6]-Phenyl-C61-butyric acid methyl ester ($PC_{61}BM$) and C_{60} (in inverted planar structure),[9-12] is used as the electron transport material (ETM). Compared with mesoscopic PSCs, planar PSCs have lower PCE and often suffer from the notorious hysteresis phenomenon of which the origin is still under debate.[13-16] So far, the highest reported PCE of planar PSCs is lower than that of the mesoscopic PSCs. In this study, we focus on the mesoscopic PSCs. Except for

the ETMs, another indispensable component of PSCs is the hole-transporting material (HTM) which is deposited on top of the perovskite layer in mesoscopic PSCs to extract holes from the perovskite layer and transport them to the anodes. The most commonly used HTM is a small molecular material, 2,20,7,70-tetrakis(N,N0-di-p-methoxyphenylamine)-9,90-spirobifluorene(Spiro-OMeTAD), which was first reported by Grätzel et al two decades ago.[17-18] The intrinsic semiconducting properties of Spiro-OMeTAD are not good for PSCs applications. After doping with the cobalt based dopants and ionic salt, Spiro-OMeTAD's semiconducting properties can be significantly improved. Mesoscopic PSCs using Spiro-OMeTAD as HTM have achieved the PCE higher than 20%.[3-5, 19-20] However, fabrication of the Spiro-OMeTAD HTM PSCs is very complex and the device's stability is sacrificed after doping the ionic salt into Spiro-OMeTAD.[21-26] Another shortage of using Spiro-OMeTAD in PSCs is its lengthy, expensive synthesis process and its purification is costive.[27] Besides Spiro-OMeTAD, many other small molecular HTMs have also been investigated for PSCs application. Good performance of the PSCs with the PCE above or close to 20% has been achieved with these small molecular HTMs. Michael Saliba et al synthesized a HTM with a simple dissymmetric fluorene–dithiophene (FDT) core substituted by N,N-di-p-methoxyphenylamine donor groups which can be easily modified. They proposed that the additional thiophene-iodine interaction may improve the holes' transfer at the FDT/perovskite interface, which achieved high performance of the PSCs with PCE of 20.2%.[28] Kasparas Rakstys et al reported four novel star-shaped

triazatruxene derivatives used as the HTM in PSCs, which achieved the best PCE of the device of 18.3%.[29] Sungmin Park et al reported a high mobility small molecular HTM, PCP-TPA, and obtained the PSCs with PCE of 17.8%.[30] Compared to small molecular HTMs, reports on polymer HTMs for PSCs are much fewer. So far, the most successful polymer HTM for PSCs is polytriarylamine (PTAA). The PCE of the polymer HTM PSC reached 20.2%.[2] Some p-type polymers, such as poly(3-hexylthiophene) (P3HT), poly-[2,1,3-benzothiadia-zole-4,7-diyl[4,4-bis (2-ethylhexyl)-4H-cyclopenta [2,1-b:3,4-b'] dithiophene-2,6-diyl]] (PCDTBT), Poly[2,6-(4,4-bis-(2-ethylhexyl)-4H- cyclopenta [2,1-b;3,4-b'] dithiophene)-alt-4,7(2,1,3-benzothiadiazole)] (PCPDTBT) and so on, are commonly used in organic photovoltaic (OPV) have also been applied into PSCs as the HTMs. Unfortunately, all these small molecular and polymer HTMs require ionic salt doping for PSCs to obtain better performance. Recently, more and more researchers are working on development of high performance dopant free small molecular HTMs [23-24, 31-34]. For example, K. Rakstys et al. developed a series of dopant-free small molecular HTMs. When used them in PSCs as the HTMs, a high PCE over 19% of the devices was obtained [35]. J. H. Heo et al. reported a dopant-free small molecular donor-acceptor-type HTMs for fabricating planar structure PSCs with the highest PCE of 17.3% [36]. There are also some reports on high performance PSCs based on dopant-free polymer HTMs, but they are rarer than dopant-free small molecular HTMs. Diketopyrrolopyrrole (DPP) based polymer without any dopants was reported to be used in PSCs with a PCE of 12.32% [37]. Recently K. Kranthiraja et al. developed

a series of additive-free conjugated polymers as HTMs in PSCs and achieved the highest PCE of 17.28% [38]. Besides, some other dopant-free polymer HTMs based PSCs were reported with the PCE less than 10% [39-41]. To further develop better dopant-free polymer HTMs, factors that influence the performance of dopant-free polymer HTMs must be explored and understood.

To achieve high HTM interface performance, the dopant-free polymers with proper HOMO and LUMO levels and charge carrier transport properties are very important. Incorporating thiazolothiazole fused rings into the backbone of polymers might be a good candidate for high performance dopant-free polymer as HTMs of perovskite solar cells because of their excellent charge carrier transport properties. Thiazolothiazole-containing copolymers have been reported used in OFET and OPV.[42-53] Sang Kyu Lee et al. reported a new thiazolothiazole-containing copolymer PCDTTz.[51] When the PCDTTz was used in OFET, the mobility was one order higher than another polymer without the thiazolothiazole units. Selvam et al. reported the thiazolothiazole-linked polymers have better OFET performance than a benzobisthiazole-linked copolymer.[48] The better performance was attributed to the better solid state molecular packing and crystallinity of thiazolothiazole-linked polymers. Thiazolothiazole-containing copolymers have been widely reported for the OFET and OPV applications. But to our best knowledge, they have not been reported to be used in PSCs.

In this work, we synthesized a series of new dopant-free polymer HTMs with similar

molecular structure, P1, P2 and P3, and studied the performance of these new polymer HTMs in PSCs. The best performance device was with the polymer P2 HTM, for which the PCE achieved 14.02%. The PCE of the PSC with P1 and P3 polymer HTMs was measured 10.26% and 8.47%, respectively. XRD and Time-Resolved Photoluminescence Measurement show that that the crystallinity of polymer HTMs is important to affect the PSCs' performance. It was showed that the PSCs based on P2 HTM have the lower bimolecular recombination rate and faster carriers injection at HTMs, which makes the PSC better performance. The stability of the PSCs with the new polymer HTMs is much better as comparing with the PSCs with Spiro-OMeTAD HTM. After storing in a N_2 filled glove box for 113 days, the device's PCE with the new polymer HTMs was measured still retained 80% of the original value.

2. Results and Discussion

2.1. Photovoltaic Performance of the Polymer HTMs

Thiazolothiazole-thiophene copolymers as the PSCs' HTMs have been studied in this work. **Figure 1** shows the molecular structures of the polymers. Polymer P1 has been reported to be used in OFET[49] [52]. It has been demonstrated high mobility and strong π-stacking, which make it a promising candidate for HTM in PSCs. Based on this basic design, we proposed two new polymers, P2 and P3, by replacing the bithiophene units with thieno [3,2-b] thiophene and dithieno [3,2-b:2',3'-d] thiophene units. The detailed synthesis procedure of the polymers is explained in the experimental section.

Figure 2 shows the schematic illustration (a) and cross sectional SEM image of a

mesocopic perovskite solar cell (PSC) based on P2 HTM. The PSC has a structure of glass/fluorine-doped tin oxide (FTO)/block layer TiO_2/mesoporous TiO_2/mixed perovskite/P2/gold. The mixed perovskite layer has a composition of $FA_{0.81}MA_{0.15}PbI_{2.5}Br_{0.45}$ (FA= formamidinium, MA= methylammonium) which was prepared by one-step method with anti-solvent (chlorobenzene).[3] [3] The P2 HTM was inserted between the perovskite layer and Au electrode by spin coating from its solution in o-Dichlorobenzene (DCB). As shown in the cross sectional SEM image, the P2 layer with thickness around 50 nm well covered the surface of perovskite layer and prevented the direct contact between perovskite and Au layer.

Table 1 and Figure 3 shows the photovoltaic performance of the PSCs based on P2 HTM. The best PCE of the PSC was measured 14.02% under the reverse voltage sweep direction. The highest PCE of the PSCs in the forward voltage sweep direction is 12.46%. We also prepared the PSCs with Spiro-OMeTAD HTM in the same batch for comparison. The detailed photovoltaic parameters of the Spiro-OMeTAD based PSCs are summarized in Table S1. The highest PCE of the Spiro-OMeTAD HTM based PSCs was 13.02% under reverse voltage sweep direction. These results indicate that the PSCs with P2 HTM without any dopant can achieve a comparable photovoltaic performance as the Spiro-OMeTAD HTM PSCs. From the J-V curve shown in Figure 3 (a), a slight hysteresis effect existed in the PSCs and led to a 1.56% PCE difference when scanning in different voltage sweep directions. The PSCs with Spiro-OMeTAD HTM also have similar hysteresis effect as shown in Table S1. The average PCE of the P2 HTM PSCs obtained from at least 20 cells is 11.80% and

13.03% for forward and reverse voltage sweep direction. Under reverse voltage sweep direction, the short circuit current density, J_{sc}, of the PSCs is 18.67 mA/cm^2 which is in good agreement with the calculated J_{sc}, 18.38 mA/cm^2, by integrating the product of measured external quantum efficiency (EQE) (see Figure 3 (b)) and AM1.5 spectrum. Figure 3 shows the box charts of photovoltaic parameters of the PSCs based on the P2 HTM. The small variation of the photovoltaic parameters demonstrates that performance of the P2 HTM is highly reproducible. These results indicate that P2 is suitable for applying in PSCs as the HTM and fabricating highly efficient PSCs.

The other two polymers, P1 and P3, were also used as the HTMs in PSCs. These PSCs have the similar structure as shown in Figure 2 (a). To do a fair comparison, the PSCs based on the different polymer HTMs were fabricated under the same conditions in the same batch. Table 2 and Figure 5 show the photovoltaic parameters and the J-V characteristics of the PSCs with the three different polymer HTMs under reverse voltage sweep direction. PSCs with P2 HTM have the best performance. Their PCE was measured 13.21%. The highest PCE of PSCs based on P1 and P3 HTMs was only measured at 10.26% and 8.47%, respectively.

2.2. Optical and Electronic Characterization of the Polymer HTMs

The measured J-V curves of the PSCs with different polymer HTMs show that P3 and P1 HTMs based PSCs have much lower V_{oc} than that of the P2 HTM based PSCs. It was suspected that the P2 HTM had better band alignment with the perovskite layer. To investigate the band alignment of the three polymers, we used UV-vis absorption

measurement and Photo-Electron Spectroscopy in Air (PESA) measurement to determine their highest energy occupied molecular orbital (HOMO) and lowest energy unoccupied molecular orbital (LUMO) levels. Figure 6 (a) shows the UV-vis absorption spectra of the three different polymer thin films deposited on glass substrates. The absorbance of the polymer HTMs was normalized to the peak value at the main absorption peak located at the wavelength of 624 nm. Another absorption peak with a vibronic absorption shoulder located at 572 nm. The absorption maxima ($\lambda_{abs,max}$) at 624 nm and 572 nm correspond to 0-0 and 0-1 transitions.[49] [52] The optical band gap (E_g) of the polymer was calculated from the onset of absorption spectra (λ_{onset}). As shown in the Table 3, the optical bandgaps of P1, P2 and P3 are 1.88 eV, 1.83 eV and 1.84 eV, respectively. The optical bandgap of P1 is the largest among the three polymers. Despite the small difference of the optical bandgap, all three polymers have similar UV-vis absorption characteristics. The HOMO levels of the polymers were determined by PESA measurement as shown in Figure 6 (b). The HOMO levels of the polymers were obtained by extrapolating the curves of emitted photoelectrons to the background level of the collected photoelectrons curves. Then E_{LUMO} of the polymers can be obtained by adding up the E_g and E_{HOMO}. The HOMO and LUMO levels of the polymers are summarized in the Table 3. All the three polymers have similar E_{HOMO} levels, around 5.20 eV, which is very close to the reported HOMO level of Spiro-OMeTAD (5.22 eV).[54] This means that the three polymers should have similar band alignment with the perovskite layer. The poor performance of the PSCs based on the P1 and P3 HTMs should not because of large

energy barriers between the perovskite layer and the HTMs.

2.3. X-Ray Diffraction Measurement

The crystallinity of the polymer HTM thin film in the PSCs can greatly influence their charge carriers' transport, thus affecting the PSCs' performance. We carried out the X-ray diffraction (XRD) measurement to study the crystallinity of the three polymers. The XRD measurement results of three polymer thin films on glass substrates are shown in Figure 7. The thickness of the polymer films for XRD measurement is about 50 nm. The broad and amorphous hump observed in the XRD theta-2-theta scan curves of the three polymers is attributed to the glass substrates. Both P1 and P3 polymers exhibited diffraction peaks at 4.38°. Different from the less discernable peaks of P1 and P3 XRD theta-2-theta scan curves, for P2 polymer, it has a sharp and prominent diffraction peak at 4.24°, indicating that the P2 polymer has better crystallinity. The better crystallinity of P2 polymer makes the charge carriers to be better extracted and transferred from the perovskite layer to the P2 HTM then to the Au electrodes in the PSCs.

2.4. Time-Resolved Photoluminescence Measurement

From the XRD measurement, it shows that P2 polymer has the highest crystallinity among the three. To study the charge carrier injection and separation behavior at the interface between the perovskite layer and the polymer HTMs, we carried out the time-resolved photoluminescence (TRPL) measurement. The samples used for this investigation were prepared by depositing the perovskite layer on the glass substrate

followed by depositing the polymer HTM to be investigated on top. The TRPL decay curves of the samples with different polymers are shown in Figure 8. It shows that the PL quenching of the glass/perovskite/P2 sample has the fastest rate. While the PL quenching rate in the glass/perovskite/P3 was the lowest. These results indicate that the charge carriers injection from the perovskite layer into the P2 polymer film is faster than into the P1 or P3 polymer layers. The efficient charge carrier injection from perovskite to P2 is in good agreement with the highest efficiency of PSCs based on P2 HTM. We also fitted the PL decay by using a bi-exponential decay function as shown below:[55]

$$I\ (t) = A_1 exp(-\frac{t}{\tau_1}) + A_2 exp(-\frac{t}{\tau_2})$$

~~The smaller time constants τ_1 is caused by the initially photogenerated intrachain excitons' migration to defects while relaxing toward lower energy states. The larger time constant τ_2 represents the exciton lifetime of perovskite.~~ The smaller time constant τ_1 represents bimolecular recombination and the larger time constant τ_2 represents the charge carriers lifetime of perovskite film [56-57]. The PL decay times and the decay amplitudes (A1 and A2) are shown in Table 4. The average PL decay times (τ_{ave}) values are calculated by using the following equation:[58]

$$\tau_{ave} = \frac{A_1\tau_1^2 + A_2\tau_2^2}{A_1\tau_1 + A_2\tau_2}$$

The τ_{ave} of glass/perovskite/P3 is 22.78 ns which is much longer than that of glass/perovskite/P2, 11.32 ns. The shorter PL decay time and faster charge transfer

rate are beneficial for efficient extraction of charge carriers from perovskite into the polymer HTM and suppressing the charge recombination at the perovskite and HTM interface. The TRPL results match with the photovoltaic performance of the PSCs with the three polymer HTMs. The higher V_{oc}, FF and J_{sc} of the PSCs with P2 HTM could be caused by the suppressed recombination of charge carrier. So, we can conclude that the good photovoltaic performance of the P2 HTM based PSCs comes from its good charge extraction. The only difference between the three polymers is on their backbone. The polymer P2 with thienothiophene units outperformed the polymer P1 with bithiophene and P3 with dithienothiophene units. The type of thiophene units on the backbone of polymer HTM should relate to charge carrier extraction properties and PL decay rates. S. Paek et al. also observed the influence of thiophene units on HTM's charge carrier extraction ability [59]. In their study, the HTM PEH-3 with bithiophene units has poorer performance than the HTM PEH-9 with thienothiophene units because of poor charge carrier extraction ability. This finding agrees with our experiment results that the thienothiophene-based P2 is better than the bithiophene P1. The good performance of thienothiophene-based HTM could be due to more compact $\pi - \pi$ stacking or ordered backbone orientation (edge-on or face-on orientation) [42] [60].

2.5. Stability

As mentioned before, one of the serious issues of using Spiro-OMeTAD as the HTM in PSCs is the requirement for adding in cobalt based and ionic salt dopants, which lead to poor stability of the PSCs. while there is no dopant needed for our P2 polymer

as the HTM in PSCs, which can improve the PSCs' stability. To study the stability of the PSCs based on P2 HTM, we stored the fabricated PSCs in a N_2 filled glovebox and kept recording their performance in a period of 113 days. At the same time, we also prepared the control devices with Spiro-OMeTAD HTM and put them in the same N_2 filled glove box. Figure 9 shows the measured PCE of the devices as a function of the measurement time. The PSCs with the P2 polymer HTMs exhibited excellent stability. After storing for 113 days, their PCE still retained 80% of the original value, changed from 13.28% to 10.52%. While for the PSCs with Spiro-OMeTAD HTMs, their PCE dropped from 12.14% to 4.84% after stored for 97 days. The J-V characteristics of the as-prepared PSCs with P2 HTMs and that of the devices stored after 113 days are shown in Figure 9 (b). The FF of the PSC retained 95% of the initial value after stored for 113 days. It shows that the P2 HTM can keep its good charge carrier extraction ability in the PSCs. We have carried out the water contact angle measurement on the three dopant-free polymer HTMs and doped Spiro-OMeTAD. The water contact angle results are shown in Figure S2. The contact angles of water on P1, P2, P3 are 103.0±1.5º, 96.0±1.0º and 101.5±1.5º, respectively. Compared with that of the dopant-free polymer HTMs, the water contact angle of the doped Spiro-OMeTAD is much smaller, which shows more hydrophilic of the dopant-free polymer HTMs. So the dopant-free polymer HTMs can effectively prevent moisture permeating into perovskite films. The stronger moisture repelling ability of the dopant-free polymer HTMs should be one of the factors that lead to the pervoskite solar cells' better stability. This stability measurement indicates that the

dopant-free P2 polymer HTM is suitable for fabrication of highly stable PSCs.

3. Conclusions

In summary, a series of new dopant-free thiazolothiazole-containing copolymers have been synthesized for the HTMs application in PSCs. The PSCs with the P2 polymer HTM was measured the highest PCE of 14.02%. After stored them in N_2 ambient for 113 days, the PSCs' PCE retained 80% of the original value. The XRD measurement shows the better crystallinity of P2 polymer than the other two polymers with the similar structure. The P2 polymer HTM also shows the best charge carrier extraction ability among the three from the TRPL measurement. The crystallinity of the polymers can be controlled by adjusting the thiophene units on the polymer backbone. The investigations show that the dopant-free P2 polymer is a promising candidate for replacing the costly Spiro-OMeTAD as the HTM in PSCs. Without the dopants, the PSCs with P2 HTM exhibited excellent stability. We hope that this study will provide guidelines to synthesize more efficient and stable dopant-free polymer HTMs for PSCs. To develop high performance PSCs, besides the energy levels of the polymer HTMs, attentions should also be paid to improve the polymer HTMs' crystallinity for better charge carrier extraction.

4. Experiment section

Materials: All reagents were used as received from Sigma-Aldrich. The polymers were prepared through Stille coupling copolymerization between

2,5-bis[5-bromo-3-(2-octyldodecyl)thiophen-2-yl]thiazolo[5,4-d]thiazole and corresponding bis-trimethylstannanyl thiophene derivatives. The detailed synthesis procedure can be found in the supporting information.

PSCs fabrication: FTO substrates were cleaned using soap water and sonicated sequentially with de-ionized water, acetone and isopropanol for 10 min each. After drying at 60 ℃ in oven for several hours, the FTO substrates were exposed to ultraviolet light and ozone for 15 min. After being exposed to ultraviolet light and ozone, a TiO_2 compact layer was spin coated from a Titanium diisopropoxide bis(acetylacetonate) solution at 6000 rpm for 30s followed by sintering at 450 ℃ for 20 min. After cooling down to room temperature, a mesoporous scaffold of TiO_2 nanoparticles was deposited by spin coating a solution of TiO_2 paste in ethanol (150 mg/ml) at 6000 rpm with an acceleration of 500 rpm/s for 30 s. The substrate with TiO_2 mesoporous layer was sintered at 500 ℃ for 20 min and then cooled to room temperature. The perovskite precursor solution was prepared by dissolving PbI_2, $PbBr_2$, CH_3NH_3Br (MABr) and $NH{=}CHNH_3I$ (FAI) in a mixed solvent of anhydrous dimethyl formamide (DMF) and anhydrous dimethyl sulfoxide (DMSO). The molar ratio of PbI_2:$PbBr_2$:MABr:FAI was 1.05:0.19:0.19:1. The volume ratio of DMF to DMSO was 4:1. The perovskite precursor solution was spin coated in a N_2 filled glovebox: first, 2000 rpm for 10 s; second, 6000 rpm for 30 s. During the spin coating process, 110 μl chlorobenzene (CB) was dropped on the spinning substrate 20 s before the end of the procedure. The substrate was then annealed at 100 ℃ for 60

min and then cooled to room temperature followed by spin coating polymer HTMs (P3, P1, P2) at 1000 rpm for 30 s on the perovskite layer. The polymer HTMs solution was prepared by dissolving 6 mg polymer in 1 ml o-Dichlorobenzene (DCB). The polymer HTM solution was heated at 70 ℃ for 15 min and filtered through a 0.45 μm PTFE filter before spin coating. The device fabrication was completed by depositing Au top electrodes on the polymer HTMs by a thermal evaporator at 2×10^{-6}mbar. The initial deposition rate was controlled less than 0.5 Å/s until 10 nm Au was deposited. The device active area was defined by a shadow mask to be 0.09 cm^2.

Characterization: The current density-voltage (J-V) characteristics were measured by a Keithley 2400 parameter analyzer under one sun solar spectrum illumination (AM 1.5G, intensity 100 mW/cm^2) from a solar simulator calibrated via a silicon reference cell. Incident photon-to-current efficiency (IPCE) measurements were conducted on PSCs under short-circuit conditions through a lock-in amplifier (SR510, Stanford Research System) at a chopping frequency of 8 Hz during illumination with a monochromatic light from a Xenon arc lamp. All the J-V characteristics and IPCE measurements were conducted in a N_2 filled glovebox. The cross section SEM image of the PSCs was taken by a scanning electron microscopy (JEOL-JSM-7600F) at an accelerating voltage of 5 kV. The absorption spectra of the polymer HTMs films were measured by a Shimadzu UV-3101PC UV-VIS-NIR Spectrophotometer.

Supporting Information

Supporting Information is available from the Wiley Online Library or from the author.

Acknowledgements

The authors would acknowledge the Ministry of Education of Singapore for fund this work, RG176/16.

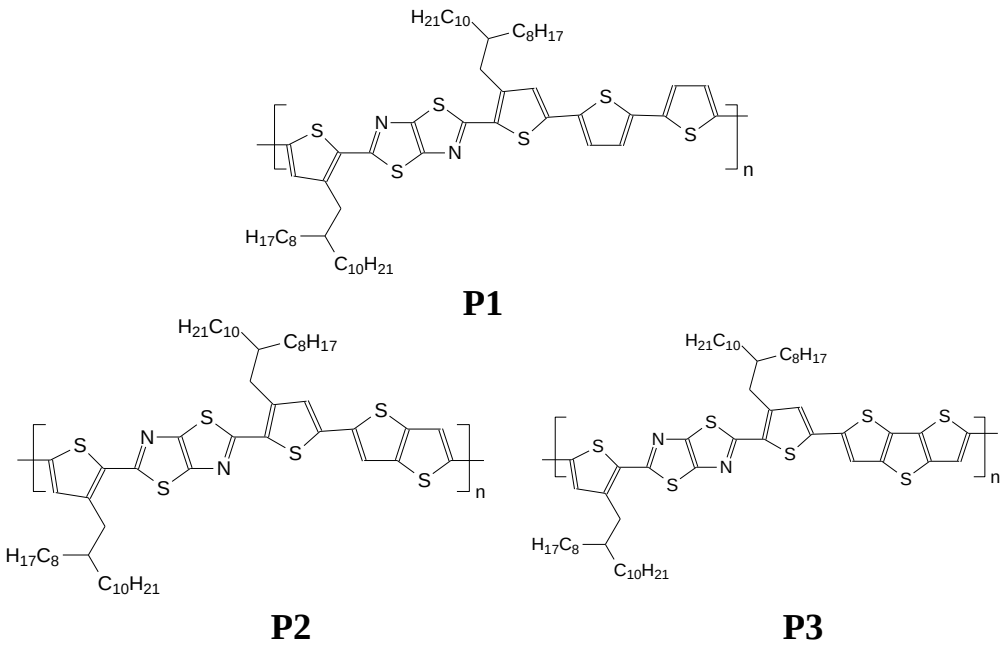

Figure 1. Molecular structures of P1, P2 and P3.

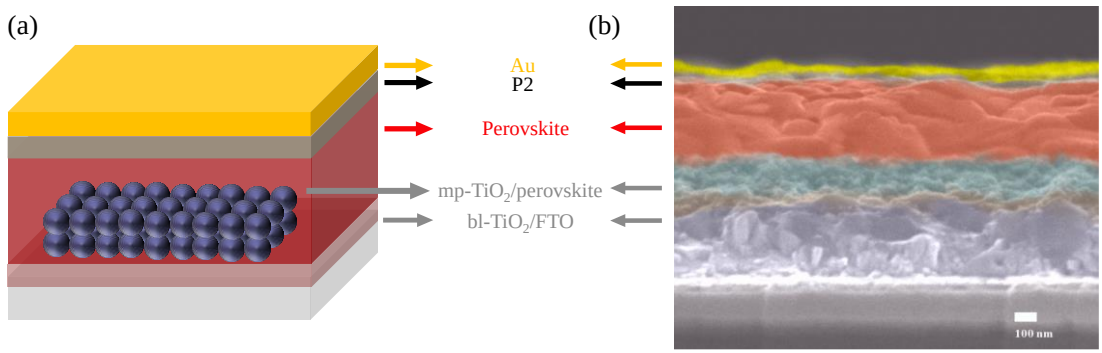

Figure 2. (a) Schematic illustration of the perovskite solar cell configuration. (b) A

high-resolution cross sectional SEM image of a complete solar cell.

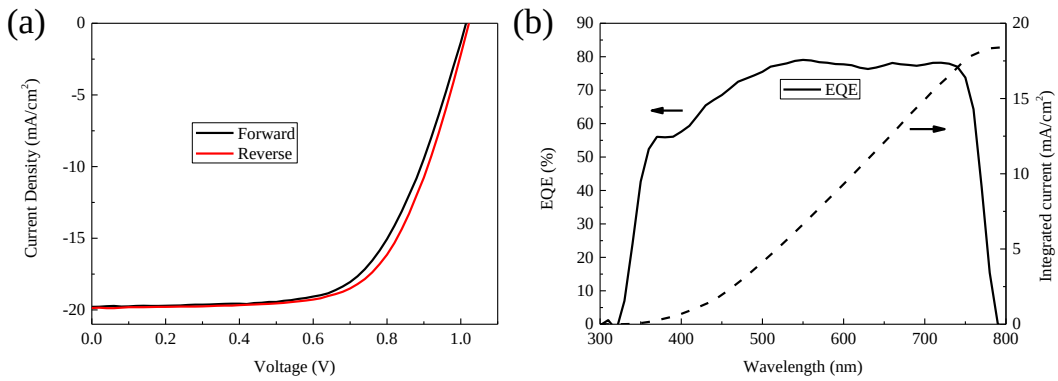

Figure 3. (a) J-V characteristics of PSCs based on P2 under forward and reverse voltage sweep directions. (b) Solid line: EQE curve of the PSCs from 300 nm to 800 nm. Dashed line: J_{sc} calculated from the overlap integral of the EQE spectrum with the standard AM1.5 solar emission.

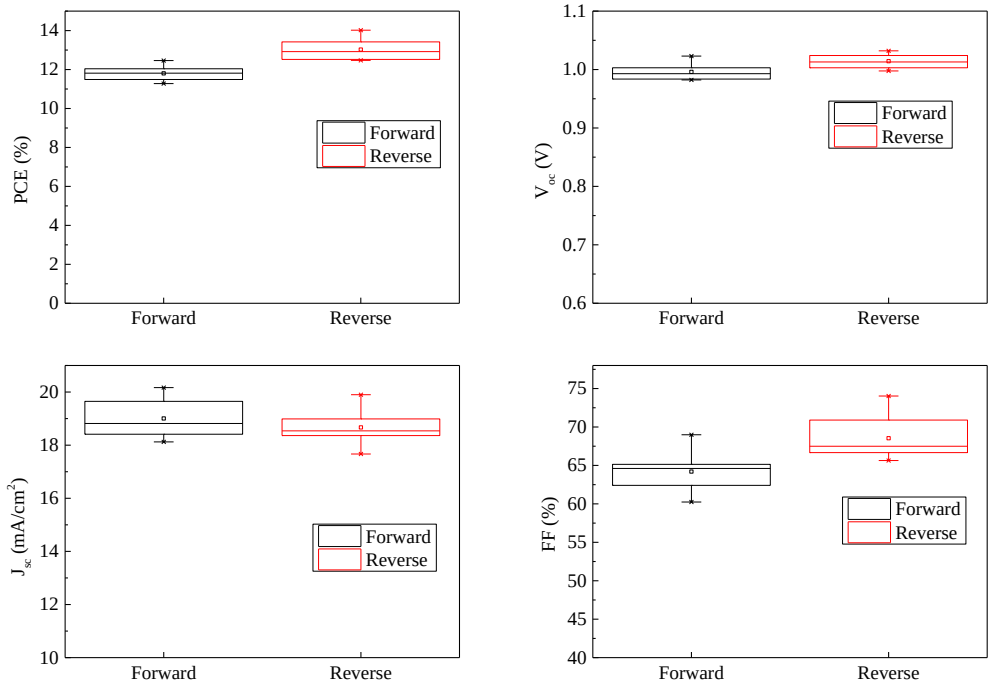

Figure 4. Box charts of the photovoltaic parameters of the PSCs based on P2 HTM.

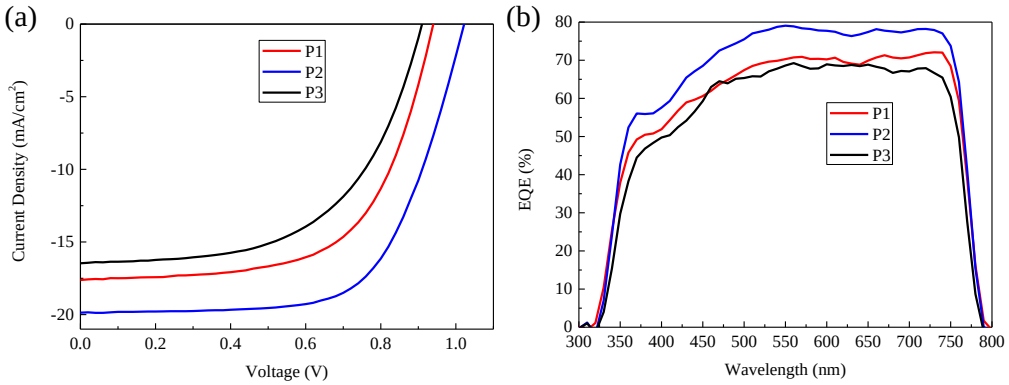

Figure 5. J-V characteristics of PSCs based on different polymer HTMs.

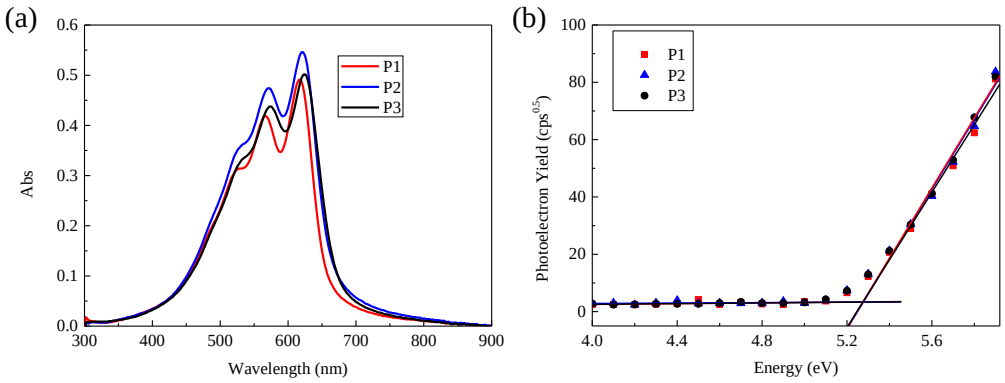

Figure 6. (a) UV-vis absorption spectra of different polymer thin films deposited on glass substrate. (b) Photoelectron spectra measured by PESA.

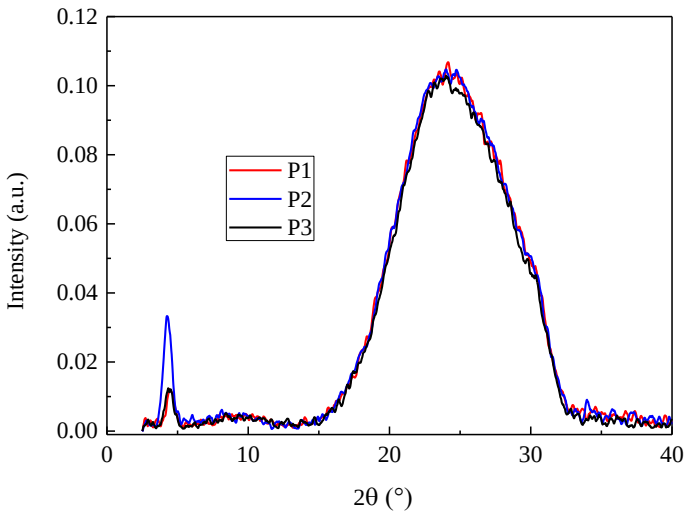

Figure 7. XRD patterns of the polymer thin films on glass substrates.

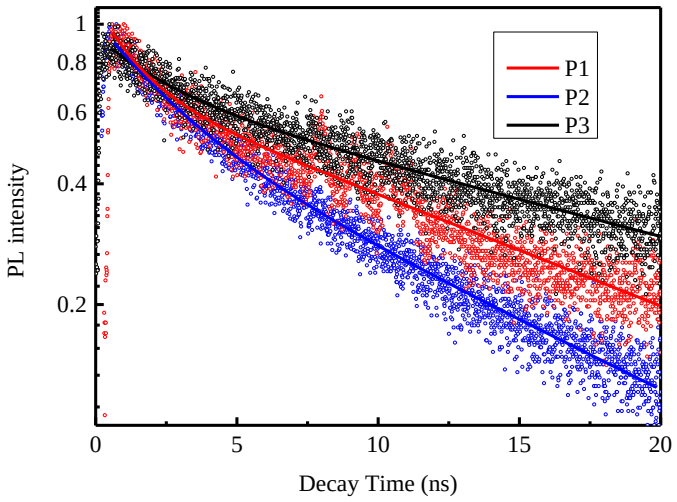

Figure 8. TRPL decay curves of glass/perovskite/HTM.

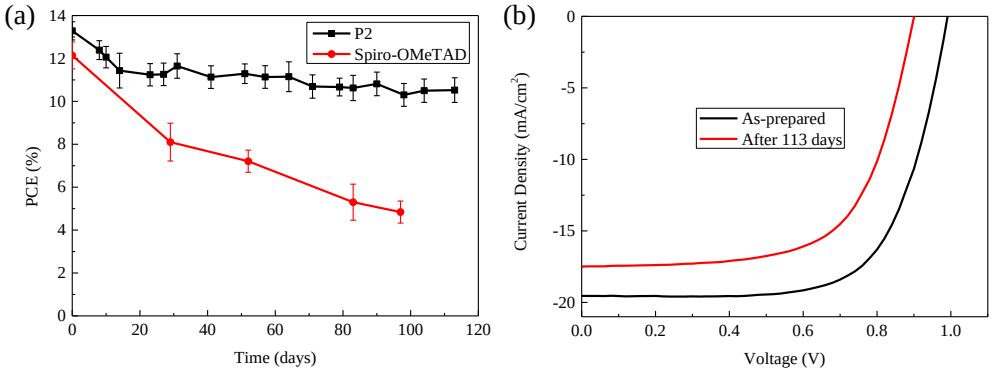

Figure 9. (a) PCE of PSCs with P2 and Spiro-OMeTAD HTMs plotted as a function of time. (b) J-V characteristics of the PSCs with P2 stored for 113 days.

Table 1. Photovoltaic parameters of the PSCs based on P2.

Voltage sweep direction	V_{oc} [V]	J_{sc} [mA/cm^2]	FF	PCE [%] Best	PCE [%] Average[a)]
Forward	1.00	19.01	0.64	12.46	11.80±0.36
Reverse	1.01	18.67	0.69	14.02	13.03±0.52

[a)]The average PCE is obtained from at least 20 cells

Table 2. Photovoltaic parameters of PSCs based on P1, P2 and P3.

HTMs	V_{oc}	J_{sc}	FF	PCE

	[V]	[mA/cm^2]		[%]
P1	0.94	17.62	0.62	10.26
P2	1.02	19.87	0.65	13.21
P3	0.90	16.47	0.57	8.47

Table 3. Optical properties and HOMO/LUMO level of HTMs

HTMs	λ_{onset} [nm]	E_{HOMO} [eV]	E_g [eV]	E_{LUMO} [eV]
P1	659.33	-5.21	1.88	-3.33
P2	678.64	-5.19	1.83	-3.36
P3	674.18	-5.20	1.84	-3.36

Table 4. Summary of the parameters from fitting to the TRPL decay data.

HTMs	A_1	τ_1 [ns]	A_2	τ_2 [ns]	τ_{ave} [ns]
P3	0.692	23.53	0.244	2.45	22.78
P1	0.713	15.63	0.408	1.42	14.93
P2	0.600	12.60	0.424	2.62	11.32

References

[1] A. Kojima, K. Teshima, Y. Shirai, T. Miyasaka, *Journal of the American Chemical Society* **2009**, 131, 6050.

[2] W. S. Yang, J. H. Noh, N. J. Jeon, Y. C. Kim, S. Ryu, J. Seo, S. I. Seok, *Science* **2015**, 348, 1234.

[3] D. Bi, W. Tress, M. I. Dar, P. Gao, J. Luo, C. Renevier, K. Schenk, A. Abate, F. Giordano, J.-P. C. Baena, *Science advances* **2016**, 2, e1501170.

[4] X. Li, D. Bi, C. Yi, J.-D. Décoppet, J. Luo, S. M. Zakeeruddin, A. Hagfeldt, M. Grätzel, *Science* **2016**, aaf8060.

[5] K. T. Cho, S. Paek, G. Grancini, C. Roldan Carmona, P. Gao, Y. H. Lee, M. K. Nazeeruddin, *Energy & Environmental Science* **2017**, DOI: 10.1039/C6EE03182J.

[6] W. Chen, Y. Wu, Y. Yue, J. Liu, W. Zhang, X. Yang, H. Chen, E. Bi, I. Ashraful, M. Grätzel, *Science* **2015**, aad1015.

[7] E. Edri, S. Kirmayer, A. Henning, S. Mukhopadhyay, K. Gartsman, Y. Rosenwaks, G. Hodes, D. Cahen, *Nano letters* **2014**, 14, 1000.

[8] W. Zhang, M. Saliba, D. T. Moore, S. K. Pathak, M. T. Hörantner, T. Stergiopoulos, S. D. Stranks, G. E. Eperon, J. A. Alexander-Webber, A. Abate, *Nature communications* **2015**, 6.

[9] W. Nie, H. Tsai, R. Asadpour, J.-C. Blancon, A. J. Neukirch, G. Gupta, J. J. Crochet, M. Chhowalla, S. Tretiak, M. A. Alam, *Science* **2015**, 347, 522.

[10] J. You, Y. M. Yang, Z. Hong, T.-B. Song, L. Meng, Y. Liu, C. Jiang, H. Zhou, W.-H. Chang, G. Li, *Applied Physics Letters* **2014**, 105, 183902.

[11] J. You, Z. Hong, Y. M. Yang, Q. Chen, M. Cai, T.-B. Song, C.-C. Chen, S. Lu, Y. Liu, H. Zhou, **2014**.

[12] W. Yan, Y. Li, Y. Li, S. Ye, Z. Liu, S. Wang, Z. Bian, C. Huang, *Nano Energy* **2015**, 16, 428.

[13] Y. Shao, Z. Xiao, C. Bi, Y. Yuan, J. Huang, *Nature communications* **2014**, 5.

[14] H. J. Snaith, A. Abate, J. M. Ball, G. E. Eperon, T. Leijtens, N. K. Noel, S. D. Stranks, J. T.-W. Wang, K. Wojciechowski, W. Zhang, *The journal of physical chemistry letters* **2014**, 5, 1511.

[15] W. Tress, N. Marinova, T. Moehl, S. M. Zakeeruddin, M. K. Nazeeruddin, M. Gratzel, *Energy & Environmental Science* **2015**, 8, 995.

[16] E. L. Unger, E. T. Hoke, C. D. Bailie, W. H. Nguyen, A. R. Bowring, T. Heumuller, M. G. Christoforo, M. D. McGehee, *Energy & Environmental Science* **2014**, 7, 3690.

[17] U. Bach, D. Lupo, P. Comte, J. Moser, F. Weissörtel, J. Salbeck, H. Spreitzer, M. Grätzel, *Nature* **1998**, 395, 583.

[18] J. Krüger, R. Plass, L. Cevey, M. Piccirelli, M. Grätzel, U. Bach, *Applied Physics Letters* **2001**, 79, 2085.

[19] M. Saliba, T. Matsui, J.-Y. Seo, K. Domanski, J.-P. Correa-Baena, M. K. Nazeeruddin, S. M. Zakeeruddin, W. Tress, A. Abate, A. Hagfeldt, *Energy & Environmental Science* **2016**, 9, 1989.

[20] T. J. Jacobsson, J.-P. Correa-Baena, M. Pazoki, M. Saliba, K. Schenk, M. Grätzel, A. Hagfeldt, *Energy & Environmental Science* **2016**, 9, 1706.

[21] Z. Hawash, L. K. Ono, S. R. Raga, M. V. Lee, Y. Qi, *Chemistry of Materials* **2015**, 27, 562.

[22] Y. K. Wang, Z. C. Yuan, G. Z. Shi, Y. X. Li, Q. Li, F. Hui, B. Q. Sun, Z. Q. Jiang, L. S. Liao, *Advanced Functional Materials* **2016**, 26, 1375.

[23] M. Franckevicius, A. Mishra, F. Kreuzer, J. Luo, S. M. Zakeeruddin, M. Gratzel, *Materials Horizons* **2015**, 2, 613.

[24] S. Kazim, F. J. Ramos, P. Gao, M. K. Nazeeruddin, M. Gratzel, S. Ahmad, *Energy & Environmental Science* **2015**, 8, 1816.

[25] C. Huang, W. Fu, C.-Z. Li, Z. Zhang, W. Qiu, M. Shi, P. Heremans, A. K.-Y. Jen, H. Chen, *Journal of the American Chemical Society* **2016**, 138, 2528.

[26] Y. Liu, Z. Hong, Q. Chen, H. Chen, W. H. Chang, Y. M. Yang, T. B. Song, Y. Yang, *Advanced Materials* **2016**, 28, 440.

[27] A. T. Murray, J. M. Frost, C. H. Hendon, C. D. Molloy, D. R. Carbery, A. Walsh, *Chemical Communications* **2015**, 51, 8935.

[28] M. Saliba, S. Orlandi, T. Matsui, S. Aghazada, M. Cavazzini, J.-P. Correa-Baena, P. Gao, R. Scopelliti, E. Mosconi, K.-H. Dahmen, F. De Angelis, A. Abate, A. Hagfeldt, G. Pozzi, M. Graetzel, M. K. Nazeeruddin, *Nature Energy* **2016**, 1, 15017.

[29] K. Rakstys, A. Abate, M. I. Dar, P. Gao, V. Jankauskas, G. n. Jacopin, E. Kamarauskas, S. Kazim, S. Ahmad, M. Grätzel, *Journal of the American Chemical Society* **2015**, 137, 16172.

[30] S. Park, J. H. Heo, C. H. Cheon, H. Kim, S. H. Im, H. J. Son, *J. Mater. Chem. A* **2015**, 3, 24215.

[31] F. J. Ramos, K. Rakstys, S. Kazim, M. Gratzel, M. K. Nazeeruddin, S. Ahmad, *RSC Advances* **2015**, 5, 53426.

[32] L. Cabau, I. Garcia-Benito, A. Molina-Ontoria, N. F. Montcada, N. Martin, A. Vidal-Ferran, E. Palomares, *Chemical Communications* **2015**, 51, 13980.

[33] Y. Song, S. Lv, X. Liu, X. Li, S. Wang, H. Wei, D. Li, Y. Xiao, Q. Meng, *Chemical Communications* **2014**, 50, 15239.

[34] S. Lv, Y. Song, J. Xiao, L. Zhu, J. Shi, H. Wei, Y. Xu, J. Dong, X. Xu, S. Wang, Y. Xiao, Y. Luo, D. Li, X. Li, Q. Meng, *Electrochimica Acta* **2015**, 182, 733.

[35] K. Rakstys, S. Paek, P. Gao, P. Gratia, T. Marszalek, G. Grancini, K. T. Cho, K. Genevicius, V. Jankauskas, W. Pisula, M. K. Nazeeruddin, *Journal of Materials Chemistry A* **2017**, 5, 7811.

[36] J. H. Heo, S. Park, S. H. Im, H. J. Son, *ACS Applied Materials & Interfaces* **2017**, 9, 39511.

[37] A. Dubey, N. Adhikari, S. Venkatesan, S. Gu, D. Khatiwada, Q. Wang, L. Mohammad, M. Kumar, Q. Qiao, *Solar Energy Materials and Solar Cells* **2016**, 145, Part 3, 193.

[38] K. Kranthiraja, K. Gunasekar, H. Kim, A.-N. Cho, N.-G. Park, S. Kim, B. J. Kim, R. Nishikubo, A. Saeki, M. Song, S.-H. Jin, *Advanced Materials* **2017**, 29, 1700183.

[39] J. Luo, J.-H. Im, M. T. Mayer, M. Schreier, M. K. Nazeeruddin, N.-G. Park, S. D. Tilley, H. J. Fan, M. Grätzel, *Science* **2014**, 345, 1593.

[40] Y. Xiao, G. Han, Y. Chang, H. Zhou, M. Li, Y. Li, *Journal of Power Sources* **2014**, 267, 1.

[41] J. W. Lee, S. Park, M. J. Ko, H. J. Son, N. G. Park, *ChemPhysChem* **2014**, 15, 2595.

[42] K. Zhao, Q. Wang, B. Xu, W. Zhao, X. Liu, B. Yang, M. Sun, J. Hou, *Journal of Materials Chemistry A* **2016**, 4, 9511.

[43] Z. Zhao, H. Liu, Y. Zhao, C. Cheng, J. Zhao, Q. Tang, G. Zhang, Y. Liu, *Chemistry–An Asian Journal* **2016**, 11, 2725.

[44] M. Saito, I. Osaka, Y. Suzuki, K. Takimiya, T. Okabe, S. Ikeda, T. Asano, *Scientific reports* **2015**, 5.

[45] S. Subramaniyan, H. Xin, F. S. Kim, N. M. Murari, B. A. Courtright, S. A. Jenekhe, *Macromolecules* **2014**, 47, 4199.

[46] I. Osaka, M. Saito, T. Koganezawa, K. Takimiya, *Advanced Materials* **2014**, 26, 331.

[47] Y. Liu, H. Dong, S. Jiang, G. Zhao, Q. Shi, J. Tan, L. Jiang, W. Hu, X. Zhan, *Chemistry of Materials* **2013**, 25, 2649.

[48] S. Subramaniyan, F. S. Kim, G. Ren, H. Li, S. A. Jenekhe, *Macromolecules* **2012**, 45, 9029.

[49] I. Osaka, M. Saito, H. Mori, T. Koganezawa, K. Takimiya, *Advanced Materials* **2012**, 24, 425.

[50] Q. Shi, H. Fan, Y. Liu, J. Chen, Z. Shuai, W. Hu, Y. Li, X. Zhan, *Journal of Polymer Science Part A: Polymer Chemistry* **2011**, 49, 4875.

[51] S. K. Lee, J. M. Cho, Y. Goo, W. S. Shin, J.-C. Lee, W.-H. Lee, I.-N. Kang, H.-K. Shim, S.-J. Moon, *Chemical Communications* **2011**, 47, 1791.

[52] I. Osaka, R. Zhang, J. Liu, D.-M. Smilgies, T. Kowalewski, R. D. McCullough, *Chemistry of Materials* **2010**, 22, 4191.

[53] X. Li, X. Tang, F. Wang, V. Chellappan, T. W. Weei, S. Guo, H. Wang, D. Wu, J. Li, *IEEE Journal of Photovoltaics* **2016**, 6, 696.

[54] N. J. Jeon, H. G. Lee, Y. C. Kim, J. Seo, J. H. Noh, J. Lee, S. I. Seok, *Journal of the American Chemical Society* **2014**, 136, 7837.

[55] Z. Zhu, Y. Bai, H. K. H. Lee, C. Mu, T. Zhang, L. Zhang, J. Wang, H. Yan, S. K. So, S. Yang, *Advanced Functional Materials* **2014**, 24, 7357.

[56] R. Zhang, C. Fei, B. Li, H. Fu, J. Tian, G. Cao, *ACS Applied Materials & Interfaces* **2017**, 9, 9785.

[57] Q. Chen, H. Zhou, T.-B. Song, S. Luo, Z. Hong, H.-S. Duan, L. Dou, Y. Liu, Y. Yang, *Nano Letters* **2014**, 14, 4158.

[58] B. Wu, K. Fu, N. Yantara, G. Xing, S. Sun, T. C. Sum, N. Mathews, *Advanced Energy Materials*

2015, 5.

[59] S. Paek, I. Zimmermann, P. Gao, P. Gratia, K. Rakstys, G. Grancini, M. K. Nazeeruddin, M. A. Rub, S. A. Kosa, K. A. Alamry, A. M. Asiri, *Chemical Science* **2016**, 7, 6068.

[60] Z. Zhao, H. Liu, Y. Zhao, C. Cheng, J. Zhao, Q. Tang, G. Zhang, Y. Liu, *Chemistry–An Asian Journal* **2016**, 11, 2725.